Accepted Manuscript

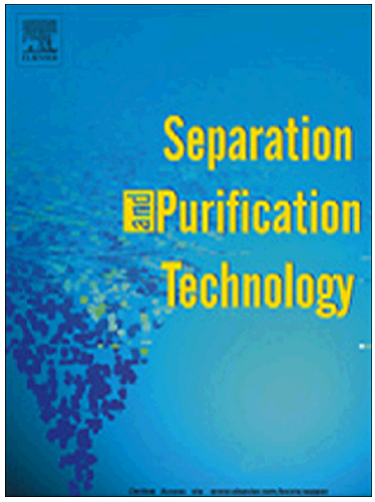

Mesoporous TiO_2 based membranes for water desalination and brine processing

Christelle Yacou, Simon Smart, João C. Diniz da Costa

PII: S1383-5866(15)00252-X
DOI: http://dx.doi.org/10.1016/j.seppur.2015.04.028
Reference: SEPPUR 12310

To appear in: *Separation and Purification Technology*

Received Date: 22 January 2015
Revised Date: 20 April 2015
Accepted Date: 20 April 2015

Please cite this article as: C. Yacou, S. Smart, J.C. Diniz da Costa, Mesoporous TiO_2 based membranes for water desalination and brine processing, *Separation and Purification Technology* (2015), doi: http://dx.doi.org/10.1016/j.seppur.2015.04.028

Mesoporous TiO_2 based membranes for water desalination and brine processing

Christelle Yacou, Simon Smart* and João C. Diniz da Costa

The University of Queensland, FIM^{2}Lab – Functional Interfacial Materials and Membrane Laboratory, School of Chemical Engineering, Brisbane, Qld 4072, Australia.

***** Author to whom correspondence should be addressed; E-Mail: s.smart@uq.edu.au ; Tel.: +61-7-3365 8591; Fax: +61-7-3365 4199.

Abstract

This work shows the preparation, characterisation and testing of TiO_2 membranes dip-coated on commercial α-Al_2O_3 tubes for desalination. TiO_2 thin films (~400 nm) were synthesised from titanium propoxide and exposed to a gentle thermal treatment to control particle and pore sizes (d_p ~ 4 nm). The TiO_2 membranes were tested for brackish (0.3 wt%), sea water (3.5 wt%) and brine concentrations (7.5 and 10 wt%) up to 75 °C in a pervaporation setup. Water fluxes as high as 10.5 kg m^{-2} h^{-1} were achieved for brackish concentrations, whilst values of up to 4.0 and 6.0 kg m^{-2} h^{-1} were measured for the highest brine concentration (10 wt%). Concentration and temperature polarisation both affected the water fluxes, particularly for brine solutions, though the latter was more dominant. Salt rejection remained very high at ~99% for all tested conditions, thus demonstrating the feasibility of mesoporous inorganic TiO_2 structures for desalination and brine processing. The TiO_2 membranes proved to be stable for long term (>350 h) testing even under thermal cycling conditions.

Keywords: desalination; brine processing; titania; mesopores**.**

1.0 Introduction

Inorganic membranes have been considered for desalination in a pervaporative operating mode at ambient conditions, thus overcoming high pressure requirements (7 MPa) seen in reverse osmosis. [1, 2]. An important characteristic of inorganic membranes is that they are conventionally engineered as asymmetric membranes. This allows for the use of ceramic substrates with large pore sizes (~0.5 μm) which provides the mechanical integrity for the membrane systems, followed by interlayers to reduce pore size to mesoporous dimensions (2 to 5 nm), and finally an ultra-microporous (<1nm) top thin layer. This type of membrane construction allows for the resistance for the transport of water to be lowest at the membrane substrate and interlayers. The control of pore size for the top thin layer is very important to allow for the diffusion of water, which has a small kinetic diameter (d_k=2.6 Å), and to reject the passage of hydrated ions with large ionic radius (e.g. Na^+: d_k = 7.2 Å and Cl^-: d_k = 6.6 Å) [3]. The advantage of this approach is that the membrane does not necessarily need to be hydrophobic, since water vapour diffusion takes place at pore sizes slightly larger than that of the water molecule.

This type of approach has been used for the development of microporous inorganic membranes for desalination primarily for zeolites and silica based materials as listed in Table 1. Duke's group [4] developed MFI zeolite membranes based on secondary ZMS-5 seed growth which improved water fluxes to 0.7 kg m^{-2} h^{-1} when increasing pervaporation temperature up to 80 °C, though these values are considered low. However, Julbe and co-workers [5] showed that zeolite membranes were unstable in long term desalination tests. This was attributed to an ion exchange mechanism between the saline water and the ions in the zeolite crystal [6]. Pure silica membranes are also known to be hydrothermally unstable, and several strategies have been pursued to improve their stability by

embedding carbonised surfactant or triblock copolymers or metal oxides in the silica matrix and by synthesizing hybrid organosilicas [7]. As shown in Table 1, all these microporous inorganic membranes generally deliver high salt rejection at improved water fluxes of values up 11.5 kg m^{-2} h^{-1} depending upon the testing conditions.

Table 1. Performance comparison of inorganic based membranes for desalination.

Membrane Type	Feed salt conc. (wt%)	Feed temp. (°C) Lower/higher	Water flux (kg m^{-2} h^{-1}) Lower/higher	Rejection (wt%) Lower/higher	Ref
Microporous					
Zeolite MFI-ZSM-5	3.8	20 – 80	0.2 – 0.7	97 – 99	[4]
Zeolite MFI-S1	3.5	20 – 75	1 – 5.1	99	[5]
Zeolite NaA	3.7	40 – 117	0.4 – 4.2	99.9 – 99.9	[8]
SiO_2 carbonized C16	3.5	25	2.1	97	[9]
Hybrid SiO_2	3.5	25	1.7	95	[10]
SiO_2 metal doped	3.5	20 – 75	0.4 – 1.2	99.9 – 99.2	[11]
Mesoporous					
Ordered hybrid SiO_2	3.5	20 – 60	6.9 – 11	99.9	[12]
Pure SiO_2	3.5	22	6.8	98	[13]
SiO_2 carbonized P123	3.5	22 – 60	2.3 – 7.8	99	[14]
Cobalt oxide SiO_2	3.5	22 – 60	4.6 – 11.3	99.7 – 99.9	[15]

Recently, Chua and co-workers reported the preparation of ordered mesoporous silica membranes delivering reasonable water fluxes and high salt rejection [12]. A more recent work from Diniz da Costa's group [14] has shown that interlayer free carbonised template silica membranes formed mesoporous carbon moieties within the silica matrix, thus conferring improved water fluxes of up to 8.5 kg m^{-2} h^{-1} at 60 ºC whilst maintaining salt rejections as high as 99.5%. In a similar approach, also very recently, interlayer free cobalt oxide silica membranes also delivered high water fluxes of 8.5 kg m^{-2} h^{-1} at 60 ºC in addition to very high salt rejections of 99.9% [15]. Hence these recent works clearly demonstrate that mesoporous inorganic membranes can also be deployed in desalination. Following this line, we would like to propose a new approach where a mesoporous interlayer can be used as a top layer for desalination application. This may be attractive as conventionally inorganic membranes are coated on supports containing interlayers. The use of interlayers as the separating medium reduces the membrane's preparation costs by no longer

requiring additional top layers, whilst also reducing the resistance to water diffusion through the membrane.

Reliable materials are required to be deployed in desalination plants, under harsh industrial conditions while exhibiting long reliable working life [16]. Among alternative membrane materials, titania (TiO_2) is very attractive due to its excellent chemical and thermal stability over a large pH ranges. Whilst TiO_2 has been mainly the focus of photocatalytic membranes for wastewater treatment, its use in desalination has been limited. Commercially available TiO_2 membranes have been applied in the pre-treatment and partial demineralization of seawater in pressure driven nanofiltration [17, 18] and ultrafiltration [19] processes only.

Here we report for the first time the preparation and desalination performance of alternative ceramic TiO_2 membrane exhibiting a mesoporous nanostructure. We investigated the sol-gel process associated with the formation of TiO_2 mesostructures. The membrane materials were characterised via X-ray diffraction (XRD), high resolution transmission electron microscopy (HR-TEM) and N_2 adsorption analysis. The membranes were tested for a range of feed salt (NaCl) concentration from brackish (0.3 wt%), sea water (=3.5 wt%), and brine (≥ 7.5 wt%) at varying temperatures up to 75 °C. The membranes performance was determined in terms of water flux and salt rejection, whilst a long term testing (>350 h) was carried out to evaluate the stability of the resultant membranes.

2.0 Experimental

2.1 Materials and membranes synthesis

All chemical reagents were obtained from commercial sources as guaranteed-graded reagents and were used without further purification. The synthesis of the starting TiO_2 sol was adapted from previous work dealing with the preparation of sol-gel derived mesoporous TiO_2 thin films [20, 21].

For this work, we slightly changed the synthesis conditions to produce the desirable thin films. Hydrolysis and condensation of titanium propoxide (TTP, $Ti(OC_3H_7)4$, 97%) was carried out in acidic condition using hydrochloric acid. TTP, H_2O, and HCl were mixed to give a molar ratio of 1:10:0.5. The sol was then aged under stirring at room temperature during 2.5 hours.

TiO_2 membranes films were dip-coated on macroporous α-Al_2O_3 tubular substrates (Ceramic Oxide Fabricates, Australia; OD = 10 mm; ID 5 mm), with a dipping time and withdrawal rate of 1 min and of 5 cm min^{-1}, respectively. The coating was applied to the outside of the tubular substrate. Subsequently, the membranes were thermally treated at 150 °C (heating rate of 1 °C min^{-1}, dwell time of 4 h) to ensure the consolidation of the TiO_2 matrix. In addition, the membranes were calcined at 350 °C (heating rate of 1 °C min^{-1}, dwell time of 2 h) to confer a gentle thermal effect on the mesostructure of the TiO_2 matrix. This cycle of dip-coating, drying and calcination was repeated four times to ensure the full coverage of the substrate. Equivalent powders were also prepared by pouring sols on large petri dishes and then thermally treated following identical procedure as above.

Structural and textural properties of the membrane material were evaluated via XRD, (Bruker D8 Advance) and N_2 sorption analysis (Tristar II 3020, Micromeritics). XRD patterns were collected at 40 kV and 20 mA using filtered Cu Kα radiation (λ= 1.5409 Å). N_2 adsorption–desorption samples were outgassed at 200 °C for 6 h. Specific surface areas and pore volume were calculated via the multi-point Brunauer–Emmett–Teller (BET) method model at relative pressures of P/P0 = 0.06–0.3. The pore size distribution for each sample was calculated using Barrett–Joyner–Halenda (BJH) theory, from the desorption branch of the isotherms. HR-TEM measurement was also performed using a transmission electron microscope (JEOL-JEM 2100) operating at 200 keV. Micrographic grids were prepared by placing a drop of diluted sample dispersion in ethanol onto a carbon-coated

copper grid and dried at room temperature. Finally microstructural investigation of the membranes layers was carried out via scanning electron microscopy analysis (FESEM JOEL 7001).

Desalination experiments were carried out using a thermally based pervaporation set up described elsewhere and schematically shown in Fig. 1 [14]. Briefly, the membrane was immersed into the open tank containing the desired feed salt solution. The pressure on the feed side was maintained at atmospheric pressure, whereas the permeate side was evacuated to < 10 kPa using a vacuum pump. The water vapour in the permeate stream was collected in liquid nitrogen cold trap during a predetermined time interval. To minimize the effect of concentration polarization on the membrane surface, the feed solution was vigorously stirred at 5000 rpm and recycled back to a larger feed tank via a peristaltic pump at a flow rate of 40 mL min^{-1}. The testing was conducted using a broad range of water salinity (NaCl) from brackish (0.3 wt%), to seawater (3.5 wt%) and brine (7.5 and 10 wt%) solutions from 20 to 75 °C.

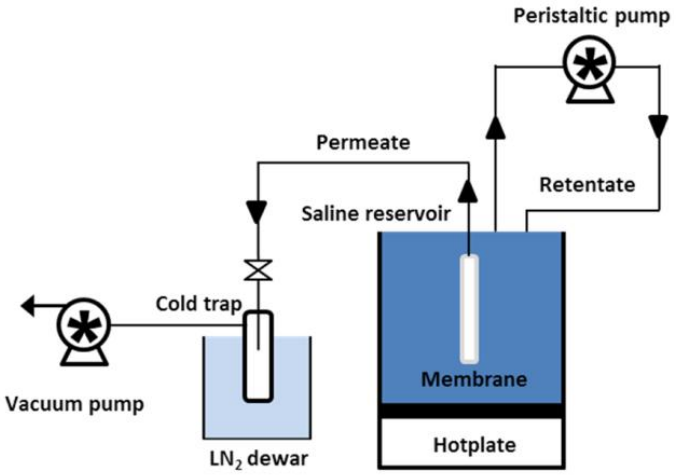

Fig. 1. A customised pervaporation set-up for membrane desalination [14].

The water flux (F) was determined based on the equation $F = m/(A \cdot \Delta t)$, where m is the mass of the permeate (kg) retained in the cold trap, A is the surface-active area (m^2) and Δt is the time interval normalised per hour (h). The salt rejection R (%) was calculated as $R = (C_f - C_p)/C_f \times 100\%$, where C_f and C_p are the feed and permeate concentrations of salt (wt %). Salt concentration of the retentate

and permeate solutions were determined by using a conductivity meter (labCHEM CP). Each test (for each salt concentration) lasted for at least 2 h to ensure a steady water flux and rejection, and then the permeate sample was collected at the predetermined time intervals. Each experimental data point reported in this work represents the average value of at least 3 permeate sample solutions.

4.0 Results and discussion

The wide-angle XRD patterns of the as-synthesized powders in Fig. 2 show broad peaks, indicating the presence of an amorphous phase or small crystalline domains formed during the sol-gel process. Upon calcination, the XRD patterns exhibit four sharp distinct peaks which are assigned to TiO_2-anatase (JCPDF 89-4121). According to Scherrer's equation, the average TiO_2-anatase crystallite sizes were approximately 8.5 (± 1.0) nm calculated from the peak width of the (1 0 1) reflection. This value is consistent with previously reported studies [22, 23].

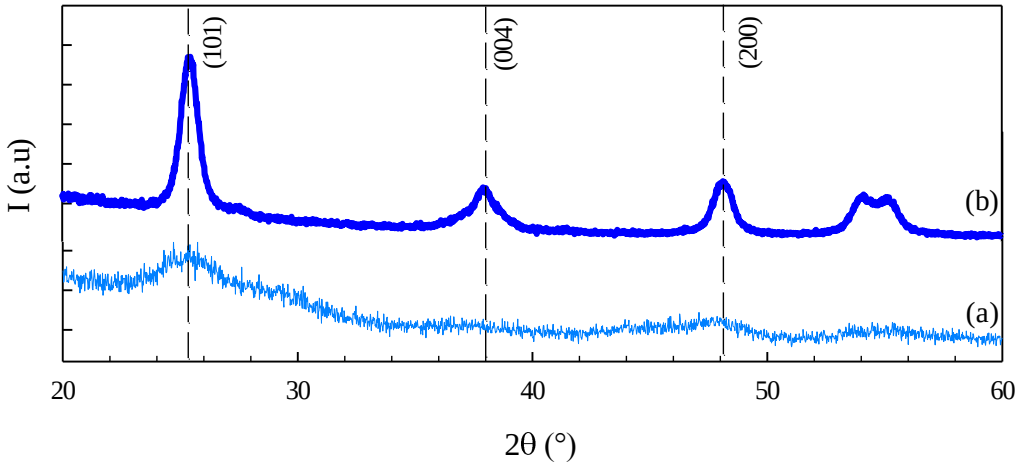

Fig. 2. XRD patterns of the as prepared (a) and calcined (b) TiO_2.

Fig. 3 displays the nitrogen isotherm of the TiO_2 membrane material. Adsorption increases in excess of p/p_0=0.2, with a minor hysteresis loop at $0.4<p/p_0<0.6$ related to the adsorption and

desorption branches. This is a classical type IV isotherm according to IUPAC classification, typical for well-developed mesoporous structures [24]. The BET surface area was calculated at 104 m^2 g^{-1}. The inset of Fig. 3 shows the pore size distribution of the TiO_2 materials determined by the BJH method from the desorption branch of the isotherm; with a mean pore diameter estimated 3.1 nm.

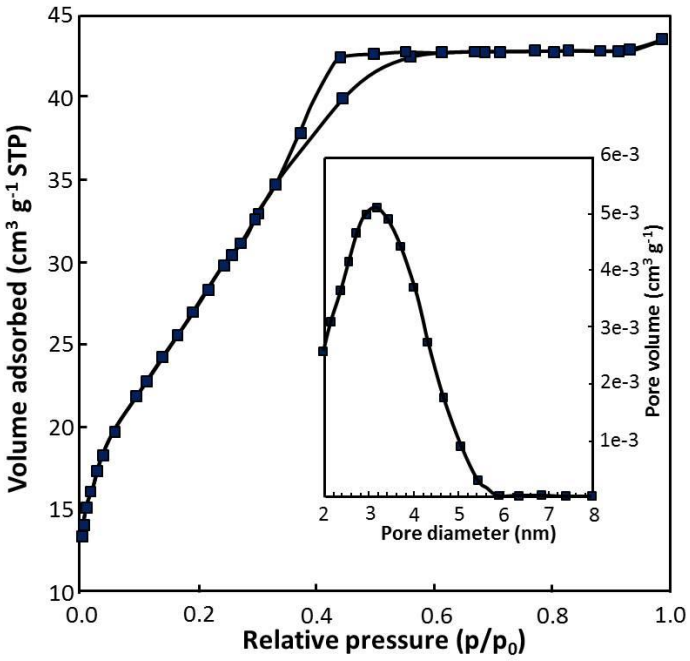

Fig. 3. N_2 sorption isotherm of TiO_2 and the associated pore size distribution (inset).

Fig. 4a displays a SEM micrograph of TiO_2 layer directly dip-coated on an α-Al_2O_3 substrate. The micrograph clearly shows a defect free TiO_2 layer, which is imperative for the fabrication of high quality TiO_2 membranes. It should be pointed out that because of the roughness of the substrate, at least four layers were necessary to fabricate a TiO_2 layer with good integrity and without cracks and pinholes. The repetition of the dip-coating procedure, necessary to achieve the desired homogeneity of the layer, led to formation of a thick symmetric TiO_2 coating layer of ~400 nm. It is also interesting to observe the partial interpenetration of the TiO_2 gel into the pores of the α-Al_2O_3 substrate up to depths of 2 μm. As the alumina particles are large (up to 0.5 μm in diameter), the inter particle large pores were partially filled by the TiO_2 gel during dip-coating. This possibly allowed for a better integration of the TiO_2 thin film on the α-Al_2O_3 substrate, thus reducing stresses

during coating and thermal calcination, and leading to the production of defect free membranes. The TEM micrograph in Fig. 4b shows several TiO_2 particles (~8nm) with clear lattice fringes. These particles are stacked on top of each other, thus making a top layer film as observed in Fig. 4a.

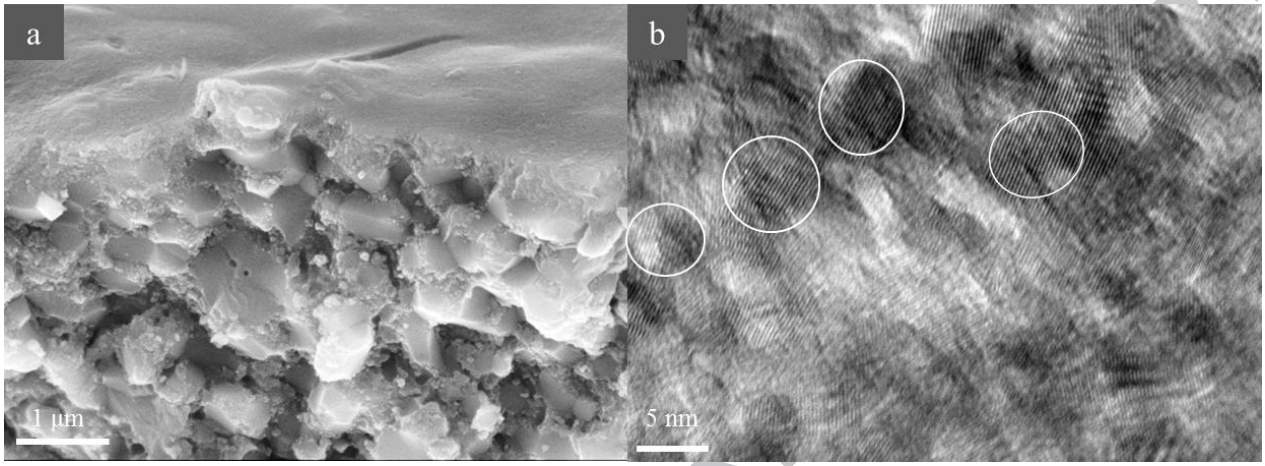

Fig. 4. (a) SEM micrograph of TiO_2 films on α-Al_2O_3 substrate cross section, and (b) TEM micrograph of TiO_2 top layer of the membrane.

The water fluxes as a function of both salt concentration and feed temperature are shown in Fig. 5a. Increasing the feed water temperature resulted in an increase in water fluxes, independently of the feed salt concentration. It is well known that the water vapour pressure increases with increasing temperature which can be predicted over typical pervaporation temperatures with the Antonie equation. As the pressure in the permeate stream is kept under vacuum (<10 kPa), the increase in the vapour pressure as a consequence of the temperature translates into a higher driving force. As the water fluxes increase as a function of the driving force, any rise in temperature leads to higher fluxes. For instance, water fluxes increased by ~220% (from 3.3 to 10.5 kg m^{-2} h^{-1}) by raising the temperature from 20 to 75 °C at 0.3 wt% salt solution. However, the driving force has increased by 1780%, from 2.04 to 38 kPa under these testing conditions. This difference could be attributed to temperature polarisation effect, as discussed in more detail below. The salt rejection remained very high with average values ~99% (Fig. 5b) irrespectively of temperature and feed salt concentration testing condition. This is interesting considering the mesoporous nature of the TiO_2 membrane.

Although the average pore sizes of 3.1 nm (±4) (Fig. 3a) are larger than 0.3-0.5 nm in molecular sieve membranes, these are still well below the pore size of 10 nm-1µm for polymeric membranes used in membrane distillation systems [25]. Hence, these results strongly suggest that mesoporous inorganic membranes can be used for desalination applications, including brine processing.

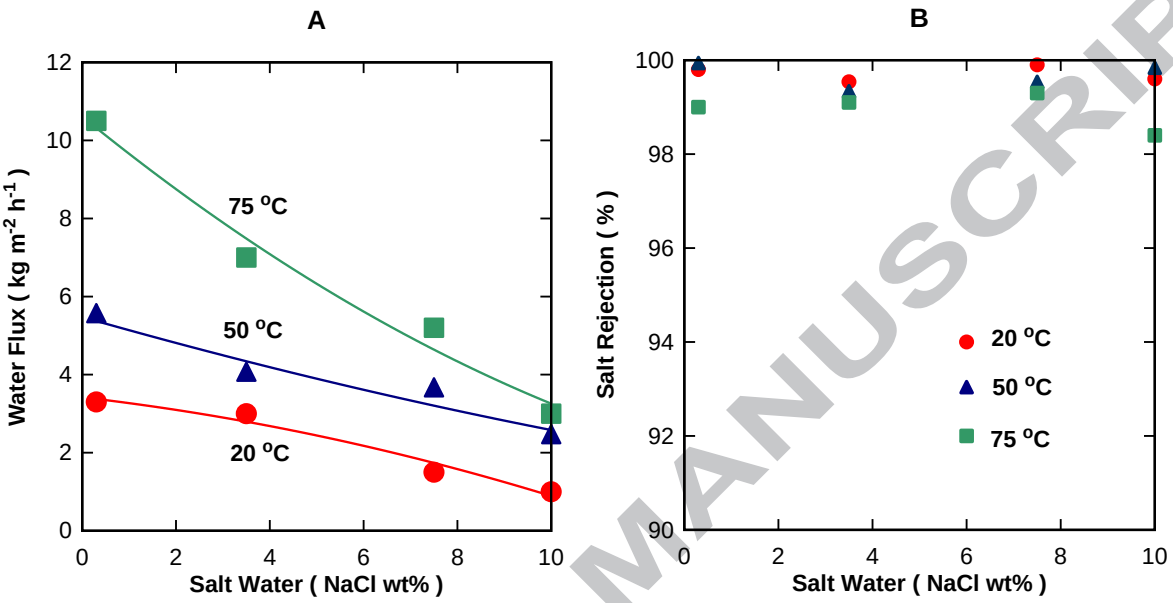

Fig. 5. TiO_2 membrane (a) water fluxes (±5%) as a function of the feed water salt concentration and (b) salt rejection (±1%). Lines are provided as a guide only.

Fig. 5a also shows that the water flux greatly reduced as a function of the feed salt concentration in the saline water. However, the change in vapour pressure driving force for an ideal salt solution is not significant, around 0.88% as the salt concentration increases for 0.3 wt% (2.3 kPa) to 3.5 wt% (2.28 kPa) [26]. Hence, this small change in the vapour pressure driving force does not justify the large reduction in water fluxes of 9% (20 °C), 27% (50 °C) and 33% (75 °C) for the same increase in salt concentration from 0.3 to 3.5 wt%. Salt concentration polarisation could be attributed to this decline as salt concentration increases in the surface of the membrane due to the fast permeation of water through the membrane. However, temperature polarisation seems to have a higher effect as the water flux reduction increases with temperature. Indeed, the Nusselt (Nu ≈ 650-900) and Sherwood (Sh ≈ 400-500) numbers calculated for the experimental setup (Re = 2.6 x 10^5) strongly

imply that temperature polarization is a more significant factor than concentration polarization [27]. However, this issue is confounded by the notion of internal concentration polarization. Recent theoretical studies have shown that the feed water can penetrate a finite distance into the pores of inorganic materials (such as mesoporous silica) operating in a manner similar to this study [28]. It is important to note the differences in membrane materials at this juncture and that pore intrusion may not occur for the TiO_2 membranes used in this study. It was certainly not observed experimentally. Regardless, if it were possible, it is easy to imagine a build-up of salt within the pores even to the point of super-saturation; however, the same theoretical analysis showed that the changes in internal concentration polarization are on the order of picomolar and therefore not significant. This is further emphasised when the minimal impact salt concentration has on the vapour pressure driving force [26]. In this work the temperature of the saline water was based on bulk temperature measurement, and not membrane surface measurement. The evaporation of water vapour in the permeate side results in cooling the membrane surface, thus causing a heat transfer where the feed membrane surface is lower than the bulk temperature of the saline water. Hence, these results strongly suggest that temperature polarisation was dominant in the reducing water fluxes.

The membranes were further tested for over 350 hours using a brackish (0.3 wt%) and brine (7.5 wt%) feed solutions as shown in Fig. 6. For the brackish processing, the water fluxes changed from 3.8 to 6.0 and 11 kg m^{-2} h^{-1} as the temperature was raised from 20 to 50 and 75 °C, respectively. These values are consistent with those measured for other membrane tested from the same batch as displayed in Fig. 5. It is noteworthy that the water flux returned to values around 4.0 kg m^{-2} h^{-1} after thermal cycling to higher temperatures up to 75 °C and back to 20 °C, thus demonstrating the thermal stability of the TiO_2 membrane. For the brine processing, the water flux drastically declined during the first testing hour from 1.8 kg m^{-2} h^{-1} to reach a minimum of 0.3 kg m^{-2} h^{-1}. This trend was not observed as the temperature increased to 50 and 75 °C, as the flux was stabilized around 4 and 6 kg m^{-2} h^{-1}, respectively. However, it is interesting to observe that the water flux continued to

vary to maximum (after cleaning) and minimum (before cleaning) values upon return to 20 °C. It was observed that salt built up on the membrane surface, especially for the higher salt concentrations at the permeate side, leading to water flux reduction. Upon salt removal by washing/cleaning the membranes with water, the fluxes recovered as shown in Fig. 6. Hence, TiO_2 mesoporous membranes can be used for processing brines, though requiring washing more frequently at every 3-4 days.

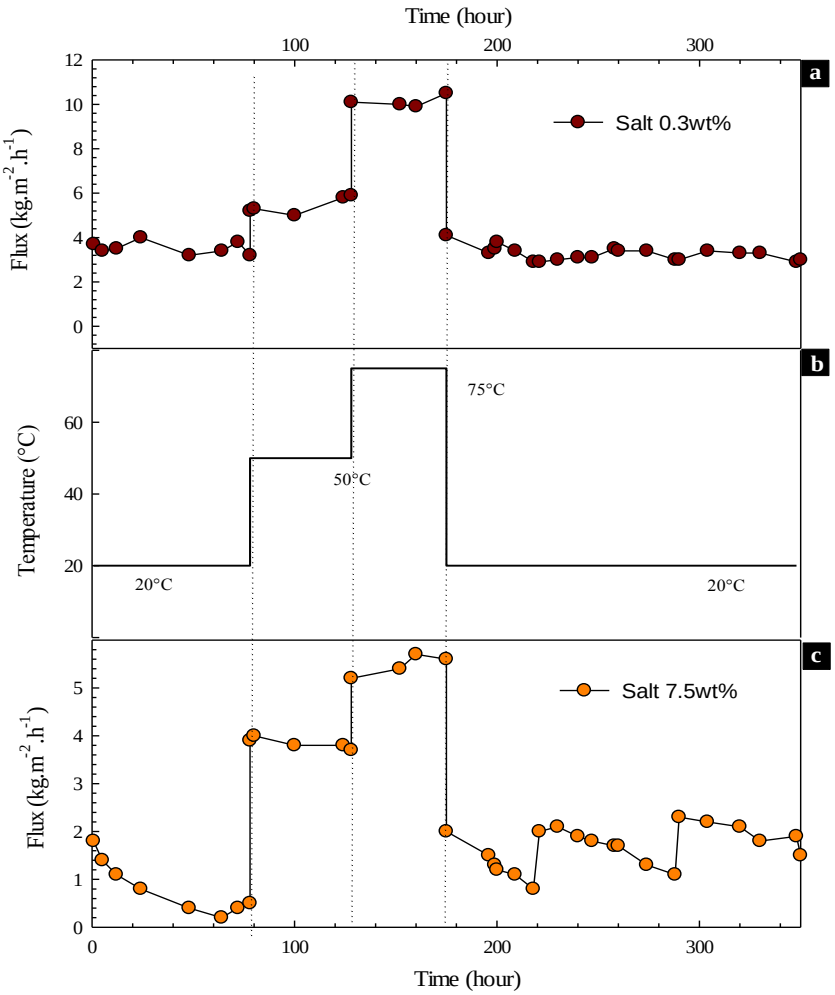

Fig. 6. 350 hours long term testing of TiO_2 membranes. Relative error of ± 5% for the water flux measurements.

Finally, the TiO_2 membranes in this work performed well, and even better, as compared to the inorganic membranes based on microporous silica or zeolites listed in Table 1. For instance, best water fluxes for the microporous carbonised silica membranes reached 3.7 kg m^{-2} h^{-1} whilst NaA

zeolite membranes reached 4.39 kg m^{-2} h^{-1} (though at very high temperatures > 100 ºC). The TiO_2 membranes also performed relatively well against the limited number of mesoporous inorganic membranes recently reported in the literature, as listed in Table 1. The water fluxes of the interlayer free P123 carbonised silica membranes [14] for brackish water were slightly lower at 8.5 kg m^{-2} h^{-1}, and in the same region for brine (7.5 wt%) as in this work. The mesoporous silica membranes results were all lower as compared with this work. It is important to note that comparing results provides a yard stick for the performance. However, testing conditions (pressures, flows and temperatures), membrane geometry (flat and tubular membranes) and substrate porosity may differ for all these membranes, so variations in results are expected.

Nevertheless, a major difference from this work as compared to all the inorganic membranes listed in Table 1 is the demonstration of mesoporous particulate TiO_2 films for desalination and brine processing, instead of amorphous silica or crystalline zeolite structures. Due to the amorphous nature of silica structures, silica membranes generally have very narrow pore size distribution, evidenced by a trimodal pore size distribution 2-3, 7-8 and 12-14Å [29]. The smaller pores tend to act as constrictions that allow the passage of the smaller molecules (i.e. water) and hinder the diffusion of the large ones (i.e. hydrated ions). This type of pore structure is also expected to be present in mesoporous silica membranes containing carbonised surfactants, though the latter tends greatly improve pore volume and conferring a membrane film structure with lower density and higher porosity than pure silica structures [14]. As a result, the carbonised silica membranes have higher water fluxes than pure silica membranes. On a similar basis adding metal oxides to silica also tend to increase pore volume and mesoporosity and water fluxes [15]. Zeolite membranes have very narrow pore size distribution such as NaA (4 Å) [30] and MFI (5.5 Å) [31], ideal for separating water from hydrated salts. However, zeolite films have tightly packed crystalline structures [32, 33] and the thickness can be up to 3-4 µm [34, 35], one order of magnitude higher than the TiO_2 film thickness of 0.3-0.5 µm observed in Fig. 4a. These structural features of zeolite membranes provide

a high resistance to water diffusion resulting in low water fluxes. Indeed, the mesoporous particulate TiO_2 films in this work differ from the structures obtained for silica and zeolites. The particles are evidenced by crystal lattice in Fig. 4b. However, this structure is also tightly packed as observed in the top TiO_2 film in the SEM image (Fig. 4a). In addition, the total pore volume as determined by N_2 adsorption of 0.066 cm^3 L^{-1} is much lower than high water flux mesoporous membranes containing cobalt oxide silica (0.186 cm^3 L^{-1}) [15] and carbonised P123 silica (0.464 cm^3 L^{-1}) [14]. Therefore, structural features play an important role in the performance of membranes, and there is a strong correlation between pore volume of the synthesised membrane films and water fluxes.

4.0 Conclusions

This work demonstrates that mesoporous TiO_2 membranes can be used for desalination and brine processing. Irrespectively of the testing condition (temperature and salt concentration), salt rejection remained always high at ~99%. Water fluxes increased with temperature, reaching values of 10.5 and 4.0 kg m^{-2} h^{-1} at 75 °C for feed waters with salt concentration of 0.3 and 10 wt%, respectively. Raising the temperature increased the partial pressure of the water vapour on the feed side, resulting in higher driving force and likewise higher water fluxes. Increasing the feed salt concentration led to a higher decrease of water fluxes than expected. This was attributed to salt concentration and temperature polarisation, the latter being the dominant factor. The TiO_2 membranes proved to be stable over 350 h of operation under varied thermal conditions. In addition, this work shows for the first time that the concept of a particulate interlayer film can be used as a separation medium in desalination applications. Thus dispensing the need of top layer requirement and increased cost production. These are important industrial requirements for the deployment of new technologies in desalination applications.

Acknowledgement

The authors gratefully thank the National Centre of Excellence in Desalination for their financial support for this project. J. C. Diniz da Costa acknowledges support from the Australian Research Council (ARC) Future Fellowship program (FT130100405). S. Smart acknowledges support from the Queensland Government Smart Futures Fellowship program. The authors would like to thank Dr Julius Motuzas and the facilities of the Australian Microscopy & Microanalysis Research Facility at the Centre for Microscopy and Microanalysis at The University of Queensland.

References

[1] C. Fritzmann, J. Löwenberg, T. Wintgens, T. Melin, State-of-the-art of reverse osmosis desalination, Desalination, 216 (2007) 1-76.

[2] L.F. Greenlee, D.F. Lawler, B.D. Freeman, B. Marrot, P. Moulin, Reverse osmosis desalination: Water sources, technology, and today's challenges, Water Res., 43 (2009) 2317-2348.

[3] J. Lin, S. Murad, A computer simulation study of the separation of aqueous solutions using thin zeolite membranes, Mol. Phys., 99 (2001) 1175-1181.

[4] M.C. Duke, J. O'Brien-Abraham, N. Milne, B. Zhu, J.Y.S. Lin, J.C. Diniz da Costa, Seawater desalination performance of MFI type membranes made by secondary growth, Sep. Purif. Technol., 68 (2009) 343-350.

[5] M. Drobek, C. Yacou, J. Motuzas, A. Julbe, L. Ding, J.C. Diniz da Costa, Long term pervaporation desalination of tubular MFI zeolite membranes, J. Membr. Sci., 415 (2012) 816-823.

[6] B. Zhu, L. Zou, C.M. Doherty, A.J. Hill, Y.S. Lin, X. Hu, H. Wang, M. Duke, Investigation of the effects of ion and water interaction on structure and chemistry of silicalite MFI type zeolite for its potential use as a seawater desalination membrane, J. Mater. Chem., 20 (2010) 4675-4683.

[7] M. Elma, C. Yacou, D.K. Wang, S. Smart, J.C. Diniz da Costa, Microporous Silica Based Membranes for Desalination, Water, 4 (2012) 629-649.

[8] C.H. Cho, K.Y. Oh, S.K. Kim, J.G. Yeo, P. Sharma, Pervaporative seawater desalination using NaA zeolite membrane: Mechanisms of high water flux and high salt rejection, J. Membr. Sci., 371 (2011) 226-238.

[9] S. Wijaya, M.C. Duke, J.C. Diniz da Costa, Carbonised template silica membranes for desalination, Desalination, 236 (2009) 291-298.

[10] M.C. Duke, S. Mee, J.C. Diniz da Costa, Performance of porous inorganic membranes in non-osmotic desalination, Water Res., 41 (2007) 3998-4004.

[11] C.X.C. Lin, L.P. Ding, S. Smart, J.C. Diniz da Costa, Cobalt oxide silica membranes for desalination, J. Colloid Interface Sci., 368 (2012) 70-76.

[12] Y.T. Chua, C.X.C. Lin, F. Kleitz, X.S. Zhao, S. Smart, Nanoporous organosilica membrane for water desalination, Chem. Commun., 49 (2013) 4534-4536.

[13] M. Elma, C. Yacou, J.C. Diniz da Costa, D.K. Wang, Performance and Long Term Stability of Mesoporous Silica Membranes for Desalination, Membranes, 3 (2013) 136-150.

[14] M. Elma, D.K. Wang, C. Yacou, J.C. Diniz da Costa, Interlayer-Free P123 Carbonised Template Silica Membranes for Desalination with Reduced Salt Concentration Polarisation, J. Membr. Sci., (2015) 10.1016/j.memsci.2014.1010.1026.

[15] M. Elma, D.K. Wang, C. Yacou, J. Motuzas, J.C. Diniz da Costa, High performance interlayer-free mesoporous cobalt oxide silica membranes for desalination applications, Desalination, 365 (2015) 308-315.

[16] T. Humplik, J. Lee, S.C. O'Hern, B.A. Fellman, M.A. Baig, S.F. Hassan, M.A. Atieh, F. Rahman, T. Laoui, R. Karnik, E.N. Wang, Nanostructured materials for water desalination, Nanotechnology, 22 (2011) 292001.

[17] T. Tsuru, K. Ogawa, M. Kanezashi, T. Yoshioka, Permeation Characteristics of Electrolytes and Neutral Solutes through Titania Nanofiltration Membranes at High Temperatures, Langmuir, 26 (2010) 10897-10905.

[18] T. Van Gestel, C. Vandecasteele, A. Buekenhoudt, C. Dotremont, J. Luyten, R. Leysen, B. Van der Bruggen, G. Maes, Alumina and titania multilayer membranes for nanofiltration: preparation, characterization and chemical stability, J. Membr. Sci., 207 (2002) 73-89.

[19] J. Xu, C.-Y. Chang, C. Gao, Performance of a ceramic ultrafiltration membrane system in pretreatment to seawater desalination, Sep. Purif. Technol., 75 165-173.

[20] C. Yacou, A. Ayral, A. Giroir-Fendler, A. Baylet, A. Julbe, Catalytic membrane materials with a hierarchical porosity and their performance in total oxidation of propene, Catal. Today, 156 (2010) 216-222.

[21] F. Bosc, A. Ayral, P.-A. Albouy, C. Guizard, A Simple Route for Low-Temperature Synthesis of Mesoporous and Nanocrystalline Anatase Thin Films, Chem. Mater., 15 (2003) 2463-2468.

[22] F. Bosc, A. Ayral, P.-A. Albouy, L. Datas, C. Guizard, Mesostructure of Anatase Thin Films Prepared by Mesophase Templating, Chem. Mater., 16 (2004) 2208-2214.

[23] T. Peng, D. Zhao, K. Dai, W. Shi, K. Hirao, Synthesis of Titanium Dioxide Nanoparticles with Mesoporous Anatase Wall and High Photocatalytic Activity, J. Phys. Chem. B, 109 (2005) 4947-4952.

[24] S. Brunauer, P.H. Emmett, E. Teller, Adsorption of Gases in Multimolecular Layers, J. Am. Chem. Soc., 60 (1938) 309-319.

[25] L. Camacho, L. Dumée, J. Zhang, J.-d. Li, M. Duke, J. Gomez, S. Gray, Advances in Membrane Distillation for Water Desalination and Purification Applications, Water, 5 (2013) 94-196.

[26] B.S. Sparrow, Empirical equations for the thermodynamic properties of aqueous sodium chloride, Desalination, 159 (2003) 161-170.

[27] F.P. Incropera, D.P. DeWitt, Fundamentals of Heat and Mass Transfer, John Wiley & Sons, New York, 1996.

[28] Y.T. Chua, G. Ji, G. Birkett, C.X.C. Lin, F. Kleitz, S. Smart, Nanoporous organosilica membrane for water desalination: Theoretical study on the water transport, J. Membr. Sci., 482 (2015) 56-66.

[29] M.C. Duke, S.J. Pas, A.J. Hill, Y.S. Lin, J.C. Diniz da Costa, Exposing the Molecular Sieving Architecture of Amorphous Silica Using Positron Annihilation Spectroscopy, Adv. Funct. Mater., 18 (2008) 3818-3826.

[30] D. Shah, K. Kissick, A. Ghorpade, R. Hannah, D. Bhattacharyya, Pervaporation of alcohol–water and dimethylformamide–water mixtures using hydrophilic zeolite NaA membranes: mechanisms and experimental results, J. Membr. Sci., 179 (2000) 185-205.

[31] Z.P. Lai, G. Bonilla, I. Diaz, J.G. Nery, K. Sujaoti, M.A. Amat, E. Kokkoli, O. Terasaki, R.W. Thompson, M. Tsapatsis, D.G. Vlachos, Microstructural optimization of a zeolite membrane for organic vapor separation, Science, 300 (2003) 456-460.

[32] A. Huang, W. Yang, J. Liu, Synthesis and pervaporation properties of NaA zeolite membranes prepared with vacuum-assisted method, Sep. Purif. Technol., 56 (2007) 158-167.

[33] Y. Morigami, M. Kondo, J. Abe, H. Kita, K. Okamoto, The first large-scale pervaporation plant using tubular-type module with zeolite NaA membrane, Sep. Purif. Technol., 25 (2001) 251-260.

[34] M. Drobek, J. Motuzas, M. van Loon, R.W.J. Dirrix, R.A. Terpstra, A. Julbe, Coupling microwave-assisted and classical heating methods for scaling-up MFI zeolite membrane synthesis, J. Membr. Sci., 401–402 (2012) 144-151.

[35] J. Motuzas, S. Heng, P.P.S. Ze Lau, K.L. Yeung, Z.J. Beresnevicius, A. Julbe, Ultra-rapid production of MFI membranes by coupling microwave-assisted synthesis with either ozone or calcination treatment, Microporous Mesoporous Mater., 99 (2007) 197-205.

Highlights

- Thin TiO_2 films without interlayers were tested for pervaporative desalination
- Fluxes up to 10.5 kg m^{-2} h^{-1} were achieved across a range of saline feeds
- Salt rejection was >99% for all testing conditions
- The membranes were stable for >350 h of testing even with thermal cycling